Linear Viscoelastic Properties of HFPE-II-52 Polyimide

J. N. Antonakakis,[1] P. Bhargava,[1] K. C. Chuang,[2] A. T. Zehnder[1]

[1]*Department of Theoretical and Applied Mechanics, Cornell University, Ithaca, New York 14853*
[2]*Polymers Division, NASA Glenn Research Center, Cleveland, Ohio 44135*

Received 4 August 2005; accepted 30 August 2005
DOI 10.1002/app.23067
Published online in Wiley InterScience (www.interscience.wiley.com).

ABSTRACT: The polyimide HFPE-II-52 was developed at NASA Glenn Research Center for use as a matrix in high temperature composite materials. The unique properties of such composites stem largely from the performance of the matrix at high temperature. Thus, as part of a larger effort to study high temperature composite materials, the linear viscoelastic properties of HFPE are measured and a mathematical model of the properties is developed. In particular, storage, loss, and stress relaxation moduli were obtained from cyclic and transient loading experiments. A Prony series was fit to the relaxation modulus data. As a cross check, the fit to the relaxation modulus was converted to storage and loss moduli and compared with those measured directly. Effects of postcuring and of moisture on the properties are investigated as well. These results provide researchers with a constitutive model for HFPE-II-52 and provide some insight into the performance of HFPE matrix composites at high temperatures. © 2006 Wiley Periodicals, Inc. J Appl Polym Sci 100: 3255–3263, 2006

Key words: high temperature materials; mechanical properties; polyimides; viscoelastic properties; Prony series

INTRODUCTION

Polymer matrix composites (PMCs) have found a broad range of applications due to their low density and high specific strength. They are applied in many weight critical systems such as automotive, aerospace, marine, and civil structures as well as in sporting goods such as skis and tennis rackets. In these applications, the material is rarely subjected to temperatures beyond 100 °C. However if new PMCs that maintain a significant fraction of their strength and stiffness at high temperatures can be developed, then the benefits of PMCs can be extended to a large range of new applications such as aircraft engines, airframes for high speed aircraft, missiles, rocket motor backup structures, and reentry vehicles.

Graphite fiber–polyimide composites are a promising class of high temperature PMCs. Such materials typically have T_g of 350–400 °C with operating temperatures of 315–370 °C.[1] In addition to high temperature capabilities, their low dielectric constants and low coefficients of thermal expansion have made polyimides suitable for electronic packaging applications.[2]

Polyimide chemistry is thought to have started at DuPont in the 1950s and 1960s,[3] with the development of Pyralin™ soluble polyimides for use as wire coatings and Kapton-H™ polyimide films. These types of polyimides, referred to as condensation polyimides, have found applications as thin films in electronics packaging, wire insulation, and gas separator membranes. In addition, condensation polyimides have been used as composite matrix resins. An example of a polyimide used in carbon fiber composites is DuPont's Avimid N®,[1] which although thermally stable, imposes difficulties in processing due to voids generated from the removal of the high boiling solvent, *N*-methyl-2-pyrrolidinone, during composite fabrication.

In the early 1970s, addition-curing polyimides were developed to improve the processability of condensation polyimides while retaining the desirable properties of stability and high temperature performance. From these efforts the polymerization of monomer reactant (PMR) family of polyimides emerged.[4] An example is PMR-15, which has a T_g of 350 °C.[5,6] Due to its good high temperature performance and processability, PMR-15 composites are widely used as lightweight components for aircraft engines for long-term (290 °C) applications.[7]

In an effort to develop a polyimide with better high temperature performance than the PMR-15, a second generation of PMR resins emerged, namely PMR-II.[8–10] Although PMR-II is inherently more thermally stable and has a higher servicing temperature of 315 °C, it is more difficult to process PMR-II than PMR-15.

These deficiencies have prompted the search for new PMR resins, with HFPE-II-52 being one of them. HFPE-II-52 replaces the norbornyl endcaps used in

Correspondence to: A. T. Zehnder (atz2@cornell.edu).
Contract grant sponsor: Constellation University Institutes Project, NASA; contract grant number: NCC3–994.

PMR-15 and PMR-II with 4-phenylethynylphthalic acid, methyl ester (PEPE)[11] endcaps. Since the phenylethynyl endcap displays a wider processing window[12] and cures without the evolution of volatile cyclopentadiene as in the case of the nadic endcap, the processability of HFPE-type resins is better than that of the corresponding PMR-II-50.

At elevated temperatures, polyimide composites will behave in a time-dependent manner because of the viscoelastic nature of the polymer matrix, changes in the chemical characteristic of the polymer (chemical aging), evolution towards an equilibrium state (physical aging), moisture absorption (hydrothermal effects), and evolving material defects due to loading and environment (damage).[13] Experimental approaches to understand the viscoelastic response and long-term behavior, coupled with damage of polyimide matrix composites are not easily developed because the large number of variables involved. Therefore, in addition to experimental methods, computational approaches based on finite element methods (FEM) are being developed and applied to understand the physical response of polyimide composites to high temperature loadings.[14] To apply these computational methods, constitutive models of all component materials, including the matrix are required. The present work aims at investigating the material properties of the polyimide HFPE-II-52. Specifically, the linear viscoelastic properties are measured over a range of −35 to 385 °C, using dynamic modulus and stress relaxation approaches. A mathematical model suitable for computational simulations is developed based on the stress relaxation modulus and cross checked against the dynamic modulus data.

THEORY

A brief review of the theory of linear viscoelasticity is given here to set the stage for the experiments and data reduction to follow. It is assumed that the material behaves in a linearly viscoelastic manner and that it follows the time–temperature superposition (TTS) principle.[15] Thus, given a uniaxial strain history $\varepsilon(t)$, the stress $\sigma(t)$ is

$$\sigma(t) = \int_0^t E(\tau - \tau')\dot{\varepsilon}(t')dt',$$

where $E(\tau)$ is the relaxation modulus, τ is time, scaled according to the TTS principle,

$$\tau = \int_0^t \frac{dt'}{a(\theta(t'))},$$

where θ is temperature and $a(\theta)$ is the scaling function. To characterize the tensile response of a linear viscoelastic material $E(t)$ and $a(\theta)$ can be determined through a series of stress relaxation experiments in which a step strain is applied to a test sample and the stress relaxation histories are measured over a wide temperature range.

An alternative is to characterize the material by its complex modulus. If at fixed temperature the strain, ε, is cycled at frequency ω and amplitude ε_0,

$$\varepsilon(t) = \mathrm{Im}[\varepsilon_0 e^{i\omega t}] = \varepsilon_0 \sin\omega t,$$

then the stress will be related to strain by

$$\sigma(t) = \mathrm{Im}[E^*(\omega,\theta)\varepsilon_0 e^{i\omega t}] = \varepsilon_0(E'(\omega,\theta)\sin\omega t + E''(\omega,\theta)\cos\omega t),$$

where

$$E^* = E' + iE''$$

is the complex modulus. The real part of E^* is the storage modulus, a measure of the energy retained during a loading cycle. The imaginary part of E^* is the loss modulus, a measure of the energy dissipated during a loading cycle. If the material was purely elastic the loss modulus would be zero.

Let $E' = E^* \cos\delta$ and $E'' = E^* \sin\delta$, where E^* is the magnitude of E^*. Using trigonometric identities the stress can be written as

$$\sigma(t) = \varepsilon_0|E^*| \sin(\omega t + \delta) = \sigma_0 \sin(\omega t + \delta).$$

Hence $E^* = \sigma_0/\varepsilon_0$ and the complex modulus can be calculated based on the measured stress amplitude, σ_0, and phase δ, as

$$E' = \frac{\sigma_0}{\varepsilon_0}\cos\delta, \qquad E'' = \frac{\sigma_0}{\varepsilon_0}\sin\delta.$$

The complex modulus is related to the stress relaxation modulus by

$$E^*(\omega,\theta) = E(\infty) + i\omega\int_0^\infty [E(\tau') - E(\infty)]e^{-i\omega t}dt'. \quad (1)$$

HFPE-II-52 SYNTHESIS AND PROCESSING

HFPE-II-52 is a polyimide prepared from a monomer solution of 4, 4′-(hexafluoroisopropylidene)diphthalic acid, methyl ester (HFDE) and *p*-phenylenediamine (*p*-PDA) with 4-phenylethynylphthalic acid, methyl ester (PEPE) in 50% methanol. Monomer reactants in methanol are commonly used to produce oligomers

terminated with reactive endcaps.[16] The aromatic endcap 4-phenylethynylphthalic acid, methyl ester (PEPE), which is used in HFPE-II-52, is known to cure at 330–395 °C without the evolution of volatiles.[17] As a result, the HFPE resin can be processed to high quality composites with a low void content. A more detailed account on how to synthesize HFPE-II-52 is provided in refs. 18 and 19.

After the HFPE-II-52 has been synthesized, it is ground into fine powder and compression molded into 100 × 100 × 3.5 mm^3 rectangular tiles. The compression molding press is first preheated to 367 °C. Then a mold is charged with 45 g of HFPE powder and placed into the press. The powder melts as the mold temperature reaches 360 °C (in about 10 min), after which a part pressure of 17.2 MPa is applied while the temperature is ramped up to 377 °C. This temperature and pressure are held for 2 h. After completion of this cycle, the pressure is removed and the part is cooled to 200 °C before removing it from the mold.

EXPERIMENTAL

Both complex modulus and stress relaxation experiments were performed. The complex modulus experiments were performed between frequencies of 0.1–100 Hz and temperature range of 25–385 °C. The stress relaxation experiments were performed at constant strain of 0.3% from −35 to 355 °C. These experiments were performed using a TA Instruments Dynamic Mechanical Analyzer DMA 2980 in three-point bending with 60 × 9×2.2 mm^3 samples. The span between support pins was 50 mm. Samples were cut with a diamond wire saw and polished to the desired thickness to a tolerance of ±0.025 mm. Samples were tested in both "dry" and "wet" conditions. The dry samples were conditioned by placing them in a vacuum oven at 70 °C for 72 h. The wet samples were conditioned by soaking in 70 °C distilled water for 72 h. Equilibrium moisture absorption is 3.2%, as measured by first drying the samples, weighing them, allowing them to saturate with moisture, and then reweighing the samples.[20]

To select the strain range for the measurements, a preliminary experiment was performed to measure the dynamic modulus as a function of strain. This experiment showed that the storage modulus at 1 Hz was independent of strain up to at least 0.5% strain. Based on these results a strain range of 0.3% was selected for all measurements.

Dynamic modulus experiments were performed at 1 Hz, using four wet and four dry samples, while a fifth pair of samples was tested over the entire temperature range at frequencies from 0.1 to 100 Hz. Each pair was taken from a different plate of HFPE-II-52. All plates were prepared from the same batch of powder. Steps of 20 °C were taken with a 5 min hold between steps to allow the sample temperature to equilibrate.

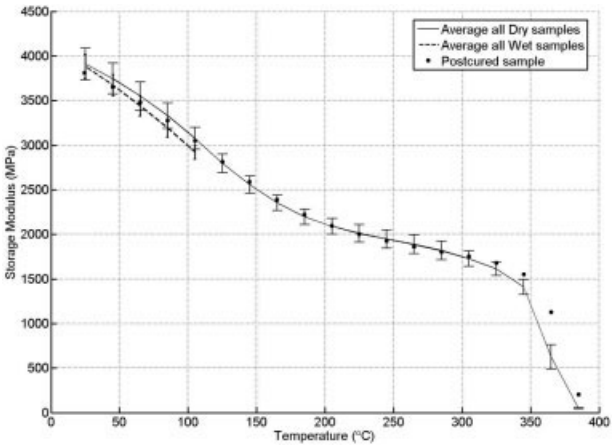

Figure 1 Average storage modulus vs. temperature of all dry and wet samples tested at 1 Hz. Each bar is 1 standard deviation. Modulus of postcured sample is plotted as well.

Stress relaxation modulus experiments were performed on two dry samples, taken from different plates. In both experiments, steps of 30 °C were taken. For the first sample, a step strain was applied and held for 20 min, while the load relaxed. Next the load was removed and the sample was allowed to recover or creep back to its initial state for 10 min. In the second sample, the relaxation and recovery times were increased to 25 and 15 min.

In addition to the above measurements, the static Poisson's ratio of the material at room temperature was measured using axial and transverse strain gauges bonded to a 100 × 13 × 2.2 mm^3 straight sample. The sample was loaded monotonically and the transverse and axial strains recorded.

RESULTS

Complex modulus

The average 1 Hz storage modulus with ±1 standard deviation error bars is plotted in Figure 1 for both dry and wet samples. The average value for the storage modulus of dry HFPE-II-52 at 25 °C is 3.91 ± 0.18 GPa. The corresponding value of storage modulus for the wet samples is 3.88 ± 0.13 GPa. The results indicate that within a standard deviation storage modulus for wet and dry samples are identical.

Note that the wet sample data are given only up to 100 °C. The samples are relatively thin and thus as they are being heated for the different temperature steps of the dynamic modulus experiment they are at the same time drying out. In a separate experiment it was found that in the ~30 min it takes to reach 100 °C during a single frequency test, the sample lost 20% of its initial moisture. In the multifrequency experiments

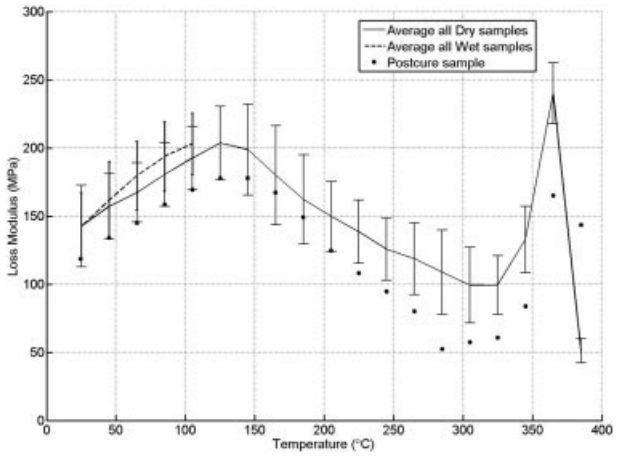

Figure 2 Average loss modulus vs. temperature of all dry and wet samples tested at 1 Hz. Each bar is 1 standard deviation. Modulus of postcured sample is plotted as well.

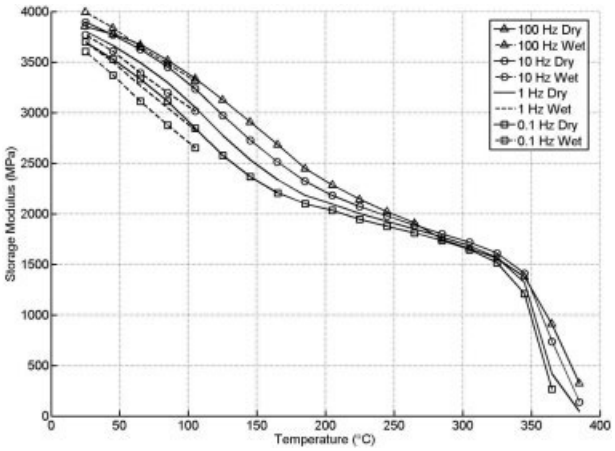

Figure 3 Storage modulus as a function of temperature for a dry and a wet sample tested at multiple frequencies. Results for 100, 10, 1, and 0.1 Hz are shown.

it takes 150 min to reach 100 °C; in that time the sample lost 50% of its moisture. Beyond 100 °C the rate of moisture loss increases further and by the time the sample reaches 200 °C it is essentially dry. Thus we are unable to report accurate wet sample data beyond 100 °C. Attempts to measure wet properties above 100 °C by rapidly heating a wet sample at 6 °C/min. failed because the sample blistered. Such behavior has been seen in earlier studies as well.[21]

The average loss modulus and error bars are plotted in Figure 2 for both the dry and wet samples. It is seen that the wet and dry samples have essentially the same loss modulus, 0.14 ± 0.03 GPa at 25 °C.

Storage modulus is a monotonically decreasing function of temperature, while loss modulus has two peaks, a beta (β) loss peak at around 135 °C and an alpha (α) loss peak at about 365 °C. The alpha loss peak is associated with the glass transition temperature (T_g) of the material. A more accurate measure of T_g was obtained using a thermomechanical analyzer, TA Instruments Q-Series 400. The glass transition temperature was determined to be 351 °C.

The effect of frequency of loading was assessed through the multifrequency experiments. The storage and loss moduli are plotted in Figures 3 and 4 for a single dry and single wet sample. As expected the storage modulus increases with frequency, although this effect is weaker at the higher temperatures. Similarly the loss modulus decreases with increasing frequency, although the decrease is relatively small.

Effect of postcuring

When fabricating PMCs, it is a standard practice to postcure the part to optimize its mechanical properties. It has been shown for HFPE that postcuring at temperatures higher than 350–370 °C, the T_g of the resin, advances the T_g of the composite. However, postcuring at temperatures higher than 371 °C for more than 40 h resulted in degradation of the neat resin.[22] To evaluate the mechanical properties of HFPE-II-52 after a typical postcure cycle, a rectangular sample of the same dimensions as the ones used for dynamic testing was heated from RT to 371 °C (700 °F) in 2 h and held at that temperature for 16 h. The postcured sample was tested for dynamic modulus at 1 Hz.

Figure 1 compares the storage modulus of the postcured sample to the average storage modulus of all dry samples. The postcured sample has a slightly lower storage modulus than average for temperatures up to about 100 °C but remains within one standard deviation, while for temperatures higher than 300 °C, its storage modulus is considerably higher. On the other hand, since Figure 2 shows that the peak of the

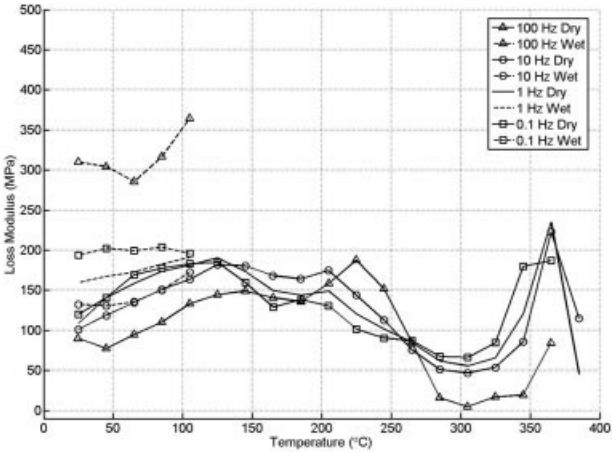

Figure 4 Loss modulus as a function of temperature for a dry and a wet sample tested at multiple frequencies. Results for 100, 10, 1, and 0.1 Hz are shown.

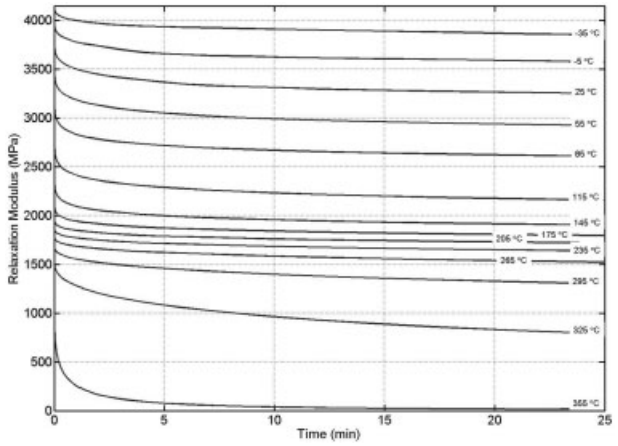

Figure 5 Relaxation modulus vs. time for sample 2.

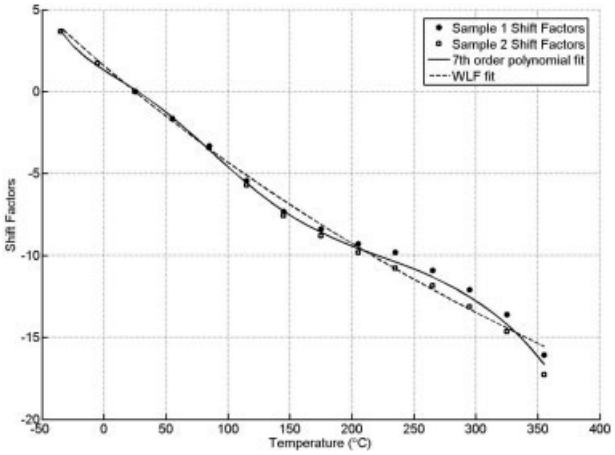

Figure 6 Shift factors, $\log_{10}(a(\theta^*))$ vs. θ^* for two samples. A polynomial and a WLF function are fit to the combined shift factors for samples 1 and 2.

loss modulus is approximately the same for the cured and postcured samples, it appears that there is no considerable increase in the T_g of the polyimide.

The effect of postcuring becomes important and desirable when the composite is intended to function in environments where the temperature is close to or beyond the glass transition temperature of the resin. For example, at 365 °C the postcured sample has a storage modulus that is 50% larger than that of the nonpostcured sample. On the other hand, postcuring may not be desirable when the operating temperature of the material is considerably below its T_g, as postcuring may result in delamination of the composite and adds considerably to the fabrication time.

Stress relaxation modulus

Stress relaxation experiments were performed for two samples. The data from the second of the two experiments are plotted in Figure 5. As expected the material relaxes much faster at high temperatures. Using the TTS principle in which time is rescaled by $\tau = t/a(\theta)$ where t is time, θ is temperature, and $a(\theta)$ the temperature-dependent scaling factor, the data can all be collected onto a single master curve by plotting the relaxation modulus versus $\log_{10}$ time and shifting the individual curves until a single smooth curve is obtained. The values of $\log_{10}(a(\theta))$ needed to shift the curves are given in Figure 6 for both samples. Shifting both data sets to 25 °C (i.e., $a(25) = 1$), the relaxation modulus is plotted against scaled time, τ, in Figure 7. Note that at the higher temperatures there is a noticeable difference between the relaxation modulus for the samples, cut from two different plates, but from the same batch of HFPE-II-52 powder. Sample 1 relaxes to a lower modulus in a shorter time, or equivalently, at a lower temperature. This is in contrast to the observation that samples made from this same plate and tested for complex modulus had higher storage moduli at every temperature.

It is interesting to note that the relaxation modulus decreases at a constant rate over a large time period and after about 10^{16} s it starts to decrease dramatically. If the material were to be used at 300 °C where $a(\theta)$ is approximately 10^{-13}, to reach $\tau = 10^{16}$ s would require $t = a(\theta) \times \tau = 10^3$ s, or just 17 min. This implies that high temperature creep rupture of composites could become an issue for relatively short durations of loading.

MATHEMATICAL MODEL

Time–temperature shift

The purpose of performing the relaxation experiment was to understand the material's properties at differ-

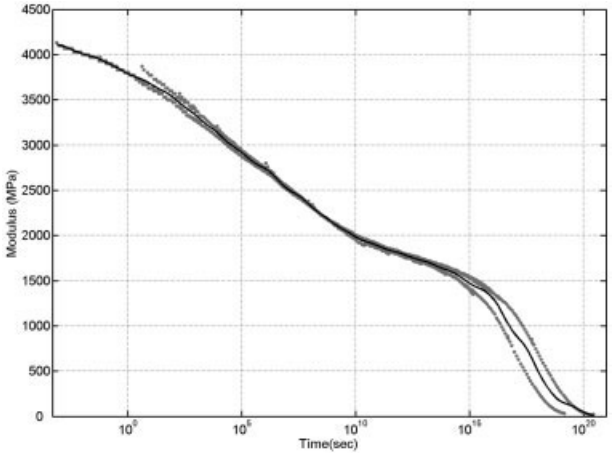

Figure 7 Relaxation modulus versus scaled time. Data from samples 1 and 2 (open circles) were individually shifted to 25°C. Nonlinear 20-term Prony series was fit (solid line) to the combined shifted data.

TABLE I
Seventh-Order Polynomial and WLF Fit Function Coefficients for Both Samples

i	7th-order polynomial fit (a_i)	WLF fit (C_i)
0	3.893	
1	−0.2634	66.25
2	6.144 E −3	1076
3	−8.456 E −5	
4	5.935 E −7	
5	−2.194 E −9	
6	4.093 E−12	θ_{ref}=25°C
7	−3.047 E−15	

ent time scales. TTS makes it possible to characterize the viscoelastic properties of a material over long time scales by obtaining data at various temperatures over an experimentally convenient time range.[15] The curve shifting procedure uses this data to create a master curve that represents the time response of a material over a wide range of times at a particular reference temperature.

The amount of shifting along the horizontal axis in a typical TTS plot required to align the individual experimental data points onto a master curve is generally described using one of two common theoretical models. The first of these models is the Williams–Landel–Ferry (WLF) equation

$$\log_{10} a(\theta) = \frac{-C_1(\theta - \theta_{ref})}{C_2 + (\theta - \theta_{ref})}$$

where C_1 and C_2 are constants, θ_{ref} is the reference temperature, θ is the measurement temperature (°C), and $\alpha(\theta)$ is the shift factor. The WLF equation is typically used to describe the time/temperature behavior of polymers in and below the glass transition region. The other model commonly used is the Arrhenius equation, which describes the behavior of a material above the glass transition temperature. However, it was found that neither the WLF nor the Arrhenius equation described the shift highly accurately, thus a 7th-order polynomial was used,

$$\log_{10} a(\theta) = a_0 + a_1^*\theta^1 + a_2^*\theta^2 + a_3^*\theta^3 + a_4^*\theta^4 + a_5^*\theta^5 + a_6^*\theta^6 + a_7^*\theta^7 \quad (2)$$

To provide two alternative approaches for $\alpha(\theta)$, the best fits to the WLF and polynomial equations are shown in Figure 6. Their coefficients are given in Table I.

Prony series for relaxation modulus

The generalized Maxwell model of the nth order of viscoelasticity for stress relaxation was used to fit the experimental data. For the relaxation modulus, $E(t,\theta)$, this takes the form[23]

$$E(t,\theta) = X_0 + \sum_{i=1}^{M} X_i e^{\frac{\alpha_i}{a(\theta)t}}, \quad (3)$$

where $E(t,\theta)$ is the relaxation modulus in shifted time domain, $t/a(\theta)$ is the shifted time, X_0 and X_i are constants to be determined, α_i are the relaxation time constants also to be determined, and M is the number of terms used.

The parameters X_0, X_i, and α_i are chosen such that the best fit to the experimental data can be achieved while remaining always positive so that basic physical and thermodynamic principles are satisfied. In physical terms the ratio of the viscosity of the dash pot to the spring rate of a Maxwell element is the relaxation time constant.

The fitting procedure follows closely that described in ref. 23, with the principal modification that the fit is fully nonlinear, i.e. X_0, X_i, and α_i are determined simultaneously rather than selecting the values of α_i ahead of time to be equally spaced in log time. It was found that the fully nonlinear approach provides a better fit for the same number of parameters, or equivalently allows one to obtain the same quality fit with fewer parameters.[19] The second change is that the Trust-Region Reflective Newton algorithm was used.[24] This algorithm, which is an improvement over the popular Levenberg–Marquardt algorithm,[25] allows a restriction on the coefficients to be imposed. In our case the coefficients X_0, X_i, and α_i are all restricted to being positive as negative stiffness and relaxation time are physically unrealistic.

As is the case in any iterative solution method, a good initial guess for the parameters to be determined is required. Following,[23] as an initial guess, the relaxation time constants are assumed to be spaced equally in log time. The constants X_0 and X_i are chosen so that the short and long behavior of the material is adequately represented. The initial guess adopted for these constants is[23]

$$X_0 = E(\tau \to \infty),$$

$$X_i = \frac{E(\tau \to 0) - E(\tau \to \infty)}{\sum_{i=1}^{N} (\tau_j)^C} (\tau_i)^C; \qquad i \in [1,N].$$

When $E(\tau \to 0)$ and $E(\tau \to \infty)$ are both of similar order of magnitude, $C = 0$ can be used. When they vary by several orders of magnitude (as with our data) a good choice for C is

$$C = 0.05 \left| \log\left(\frac{E(\tau \to 0)}{E(\tau \to \infty)}\right) \right|.$$

TABLE II
Parameters X_0, X_i, and α_i of the 20-Term Nonlinear Prony Series

Term	X_i (Pa)	α_i (s^{-1})
0	1.035 E +07	
1	1.185 E +08	2.978 E +02
2	8.632 E +07	1.638 E +01
3	1.473 E +08	1.937 E +00
4	1.348 E +08	1.188 E −01
5	1.890 E +08	8.335 E −03
6	2.001 E +08	8.931 E −04
7	2.244 E +08	7.927 E −05
8	2.244 E +08	7.011 E −06
9	2.849 E +08	2.665 E −07
10	2.181 E +08	1.411 E −08
11	1.836 E +08	1.573 E −09
12	1.675 E +08	1.510 E −10
13	1.091 E +08	1.011 E −11
14	9.777 E +07	6.190 E −13
15	1.038 E +08	3.704 E −14
16	1.898 E +08	1.825 E −15
17	4.915 E +08	3.277 E −17
18	4.462 E +08	1.639 E −18
19	3.449 E +08	3.275 E −19
20	1.651 E +08	1.498 E −20

The results of this fitting process are summarized in Table II and shown in Figure 7. It was found that the R^2 value, a measure of the goodness of the fit, did not improve significantly after 13 terms. However, when using the Prony series fit to calculate loss modulus, it was found that a 20-term fit yielded substantially better agreement and thus is used in what follows.

Cross check against dynamic modulus

To test the validity of the Prony series, the dynamic modulus was calculated based on the model equations and plotted against the experimental data. To convert from the Prony series to dynamic modulus, eq. (1) is evaluated using the Prony series for $E(t,\theta)$, eq. (3), which upon evaluation yields

$$E^*(\omega,\theta) = X_0 + \sum_{i=1}^{N} \frac{X_i \omega^2 a^2(\theta)}{\alpha_{i2} + \omega^2 a^2(\theta)} + i \sum_{i=1}^{N} \frac{X_i \omega a(\theta) \alpha_i}{\alpha_i^2 + \omega^2 a^2(\theta)} \tag{4}$$

Thus, if the Prony Series representation of the material's relaxation modulus is known, then the complex modulus is also known. The real part of the above expression corresponds to the storage modulus, and the imaginary part to the loss modulus.

The storage and loss moduli calculated from the above expression using eq. (2) for $\alpha(\theta)$ are plotted in Figures 8 and 9 along with those obtained directly from DMA dynamic experiments at 1 Hz. It is seen that the Prony series parameters fit yields a storage modulus which agrees closely with the experimentally obtained one. The calculated storage and loss moduli are plotted in Figures 10 and 11 along with those obtained directly from DMA dynamic experiments for multiple frequencies. Again there is excellent agreement between the two with the exception of the higher frequencies at temperatures above 150 °C.

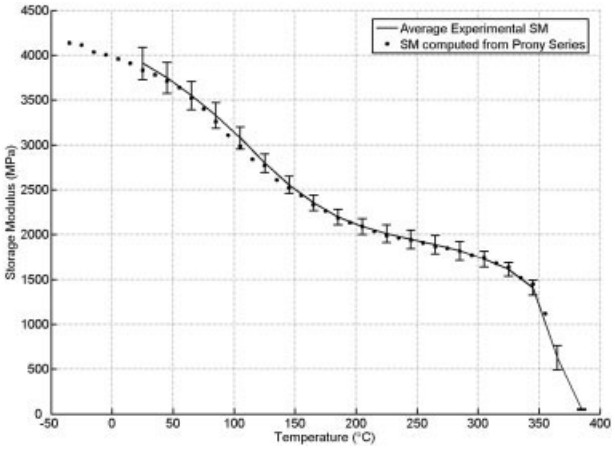

Figure 8 Storage modulus calculated from eq. (4), using the Prony series fit to the relaxation modulus along with the storage modulus obtained directly from dynamic experiments at 1 Hz.

Estimating shear modulus and Poisson's ratio

A complete viscoelastic characterization of an isotropic material requires the measurement of two properties, tensile modulus, and Poisson's ratio, for example, or shear modulus and bulk modulus as another example. Typically, the bulk modulus varies much less than the tensile and shear moduli and if one assumes that

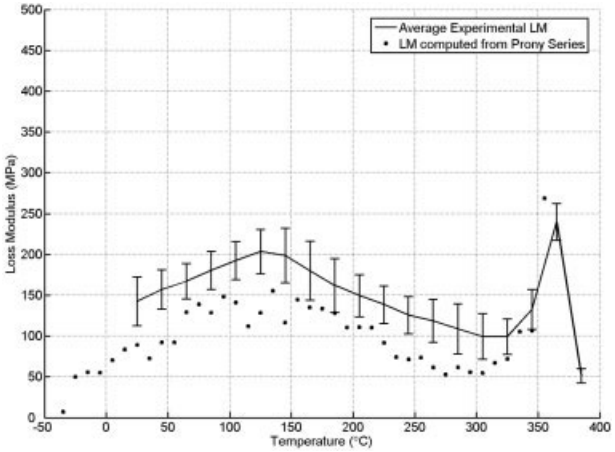

Figure 9 Loss modulus calculated from eq. (4), using the Prony series fit to the relaxation modulus along with loss modulus obtained directly from dynamic experiments at 1 Hz.

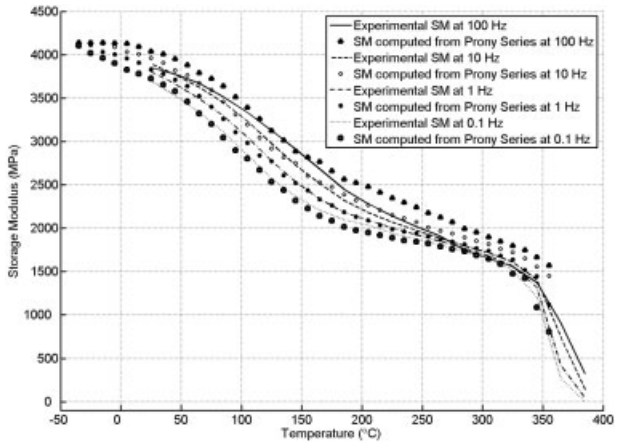

Figure 10 Storage modulus calculated from relaxation modulus fit and storage modulus obtained directly from dynamic experiments at multiple frequencies.

the bulk modulus is constant, then the Poisson's ratio and shear modulus can be determined based on the tensile relaxation modulus.

To estimate the bulk modulus a tensile experiment was performed in which axial and transverse strain gauges bonded to a tensile sample were used to measure the tensile modulus, E, and Poisson's ratio, ν. At 25 °C and a strain rate of approximately 10^{-3} s^{-1}, $E = 3.70 \pm 0.04$ GPa, and $\nu = 0.32 \pm 0.01$ were obtained. Thus the bulk modulus is estimated to be

$$K = \frac{E}{3(1-2v)} = \frac{3.67\ \text{GPa}}{3(1-2\cdot 0.32)} = 3.38 \pm 0.07\ \text{GPa}.$$

In this case the dynamic Poisson's ratio can be calculated as[26]

$$v^*(\omega,\theta) = \frac{1}{2} - \frac{E^*(\omega,\theta)}{6K}.$$

and the dynamic shear modulus as

$$G^*(\omega,\theta) = \frac{3E^*(\omega,\theta)}{9 - E^*(\omega,\theta)/K}.$$

The real part of the Poisson's ratio varies from approximately 0.3 at room temperature (1 Hz) to 0.45 at 350 °C. Note that better estimates of G and ν can be obtained if the bulk modulus is measured independently.[27] Note also that such interconversions are known to be error sensitive.[28] Further details associated with Poisson's ratio and interconversions of properties can be found in refs. 26–30.

SUMMARY AND CONCLUSIONS

The polyimide HFPE-II-52 was developed for use as the matrix material of high temperature graphite fiber reinforced composites. As potential uses of the material may be close or to even above its T_g, knowledge of the high temperature properties of HFPE-II-52 is very important to potential users of the material. In addition, since potential polyimide composite structures may be exposed to high humidity, the impact of moisture on the properties is studied. Thus a series of measurements intended to characterize the linear viscoelastic properties of the material and to assess the impact of moisture and postcuring on the material were carried out.

A total of five dry and five wet samples were tested at a frequency of 1 Hz, with one of these pairs tested at multiple frequencies ranging from 0.1 to 100 Hz, from room temperature up to 385 °C. Therefore, samples were preconditioned either as completely dry, or wet. Storage and loss moduli were obtained from these dynamic experiments. It was found that wet samples, defined as more than 95% moisture saturated, would loose as much as 50% of their moisture content by the time the temperature reached 100 °C for the heating rates used (0.5–2.5 °C/min). Thus, wet results are given for temperatures only up to 100 °C.

The average value for the storage modulus of dry HFPE-II-52 at 25 °C, 1 Hz, was found to be 3.91 ± 0.18 GPa. The corresponding value of storage modulus for the wet samples is 3.88 ± 0.13 GPa. It was observed that dry and wet samples have approximately the same value of storage modulus. From multifrequency tests it was observed that higher frequencies resulted in higher values of storage modulus regardless of moisture content in the material.

The average value for the loss modulus of dry HFPE-II-52 at 25 °C is 0.14 ± 0.03 GPa. The corresponding value of loss modulus for the wet samples is 0.14 ± 0.03 GPa. Therefore, from the experimental data collected at room temperature, both dry and wet

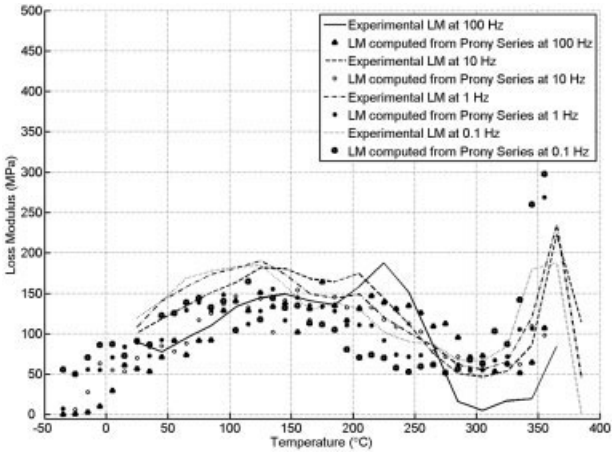

Figure 11 Loss modulus calculated from relaxation modulus fit and loss modulus obtained directly from dynamic experiments at multiple frequencies.

samples on average have the same value of loss modulus. The multifrequency tests showed that the loss modulus decreases with increasing frequency. On a molecular basis this may correspond to the absence of any molecular or atomic adjustments capable of dissipating energy within the period of deformation.

Polyimide composite materials may be loaded for long periods of time at elevated temperatures. Thus, to understand the matrix's response under such conditions, stress relaxation experiments were performed on two samples and the principle of TTS was used to obtain the relaxation modulus as a function of time. A Prony series was then fit to the relaxation versus time data. Results of the fit are tabulated in Tables I and II. As a cross check between the results obtained from dynamic and transient experiments, the result of the Prony series fit was used to convert from relaxation modulus to storage and loss moduli. The later were plotted against the experimental values of storage and loss moduli obtained directly from experiments. There was good agreement between the two.

Postcured samples had essentially the same properties as normally cured samples, the important exception being that at 365 °C the storage modulus of the postcured sample was twice that of the normally cured samples. This shows that postcuring can provide an additional margin of operating temperature.

The results presented here provide researchers with a constitutive model for HFPE-II-52, which can be used in FEA simulations that complement experimental approaches to understanding the viscoelastic response and long-term behavior of polyimide matrix composite materials.

The authors are grateful to Mr. Drew Eisenberg for performing the Poisson's ratio measurements.

References

1. Bowman, C. L.; Sutter, J. K.; Thesken, J. C; Rice, B. P. Proceedings of International SAMPE Symposium and Exhibition, 2001; Vol. 46, p 1515.
2. Matsuura, T.; Hasuda, Y.; Nishi, S.; Yamada, N. Macromolecules 1991, 24, 5001.
3. Sroog, C. E.; Endrey, L. A.; Abramo, S. V.; Berr, C. E.; Edwards, W. M.; Olivier, K. L. J Polym Sci Part A: Gen Pap 1965, 3, 1373.
4. Sroog, C. E. Prog Polym Sci 1991, 16, 561.
5. Serafini, T. T.; Delvigs, P.; Lightsey, G. R. J Appl Polym Sci 1972, 16, 905.
6. Serafini, T. T.; Delvigs, P.; Lightsey, G. R. NASA-CASE-LEW-11325–1, Patent-3 745 149 (1973).
7. Meador, M. A. Proceedings 40th International SAMPE Symposium and Exhibition, 1995; Vol. 40, p 268.
8. Serafini, T. T.; Vannucci, R. D.; Alston, W. B. NASA Report TM-X-71894, E-8680 (1976).
9. Serafini, T. T.; Cheng, P. G.; Ueda, K. K.; Wright, W. F. Proceedings of 22nd International SAMPE Technical Conference, 1990; Vol. 22, p 96.
10. Russell, J. D.; Kardos, J. L. Proceedings of 41st International SAMPE Symposium, 1996; Vol. 41, 120.
11. Chuang, K. C.; Waters, J. E.; Hardy-Green, D. Proceedings 42nd International SAMPE Symposium and Exhibition, 1997; p 1283.
12. Hou, T. H.; Jensen, B. J.; Hergenrother, P. M. J Compos Mater 1996, 30, 109.
13. Kumar, R. S.; Talreja, R. Mech Mater 2003, 35, 463.
14. Rupnowski, P.; Gentz, M.; Sutter, J. K.; Kumosa, M. Acta Mater 2004, 52, 5603.
15. Pipkin, A. C. Lectures on Viscoelasticity Theory; Springer-Verlag: Berlin, 1986.
16. Harmston, D. Proceedings of 40th International SAMPE Symposium and Exhibition, 1995; Vol. 40, p 1113.
17. Serafini, T. T.; Delvigs, P. Appl Polym Symp 1973, 2, 89.
18. Chuang, K. C.; Papadopouls, D. S.; Arendt, C. P. Proceedings 47th International SAMPE Symposium and Exhibition, 2002; p 1175.
19. Antonakakis, J. N. M.S. Thesis, Cornell University, August 2005.
20. Bhargava, P.; Chuang, K. C.; Chen, K.; Zehnder, A. T. J Appl Polym Sci 2006, submitted.
21. Rice, B. P.; Lee, C. W. 29th International SAMPE Technical Conference, 2004; p 675.
22. Chuang, K. C.; Bowman, C. L.; Tsotsis, T. K.; Arendt, C. P. High Perform Polym 2003, 15, 459.
23. Bradshaw, R. D.; Brinson, L. C. Mech Time-Dependent Mater 1997, 1, 85.
24. Branch, M. A.; Coleman, T. F.; Li, Y. SIAM J Sci Comput 1999, 21, 1.
25. Press, W. H.; Flannery, B. R.; Teukolsky, S. A.; Vetterling, W. T. Numerical Recipes, The Art of Scientific Computing; Cambridge University Press, 1989.
26. Sane, S. B.; Knauss, W. G. Mech Time-Dependent Mater 2001, 5, 325.
27. Arzoumanidis, G. A.; Liechti, K. M. Mech Time-Dependent Mater 2003, 7, 209.
28. Tschoegl, N. W.; Knauss, W. G.; Emri, I. Mech Time-Dependent Mater 2002, 6, 3.
29. Lu, H.; Zhang, X.; Knauss, W. G. Polym Eng Sci 1997, 37, 1053.
30. Mead, D. W. J Rheol 1994, 38, 1769.